Pd deposition on TiO$_2$(110) and nanoparticle encapsulation

Michael Bowker & Ryan Sharpe

Pd deposition on TiO_2(110) and nanoparticle encapsulation

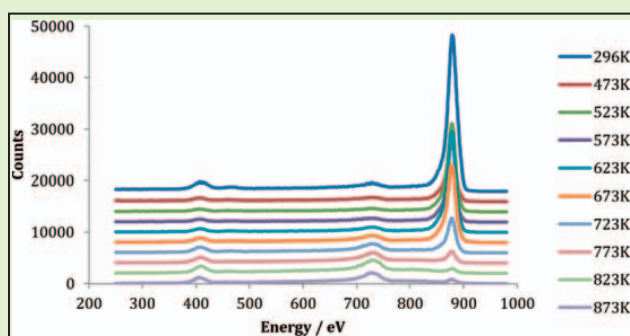**Michael Bowker**[*,1,2] and **Ryan Sharpe**[1]

[1]Cardiff Catalysis Institute, School of Chemistry, Cardiff University, Cardiff CF10 3AT, UK
[2]UK Catalysis Hub, Research Campus at Harwell (RCaH), Rutherford Appleton Laboratory, Harwell, Oxon, OX11 0FA, UK

Abstract The effect of sputtering, annealing and oxidation on the surface properties of TiO_2(110), and on the same surfaces with nanoparticles present, has been investigated. Sputtering the crystal clean gives a much reduced surface with Ti^{2+} as the dominant species. This surface is mainly $Ti^{3+,4+}$ after annealing in vacuum. Oxidation reduces the surface Ti^{3+} considerably. When Pd nanoparticles are annealed on any of the investigated titania surfaces, the particles become encapsulated by a film of titanium oxide. This is

particularly noticeable in ion scattering spectroscopy (ISS) where the Pd:Ti ratio drops by a factor of 300 after annealing to 750 K, indicating complete coverage of the Pd nanoparticles by the oxide film. This happens most easily for the nanoparticles deposited on the reduced surfaces (beginning at ~673K) but also occurs for the very oxidized surface at ~773 K. Thus, reduced Ti from the subsurface region can migrate onto the Pd surface to form the sub-oxide, the sub-oxide being a thin TiO-like layer.

Introduction

The nature of the surface of titania has become of great interest in the last 25 years[1] because of its use in a variety of applications, especially in surface treatments, coatings with special properties and, particularly with respect to the current paper, in catalysis. As regards the latter it is of considerable importance in photocatalysis, titania still being the most photo-hydro-stable material for light absorption and utilization. Many other possible photocatalysts with narrower band gaps, which would allow them to work in the visible (CdS for instance) oxidize and corrode in the presence of light. When metal nanoparticles are deposited on them, such photocatalysts have been shown to be active for sacrificial water splitting (in which holes are trapped by a sacrificial organic such as methanol[2,3]) and hydrogen production.[2-11]

There is also an important effect in catalysis called SMSI (the strong metal–support interaction), which is usually detrimental to the catalyst performance, and generally occurs for transition metal nanoparticles anchored onto reducible supports after high-temperature (~600K +)

reduction. In relation to the current paper, this is because of the encapsulation of the metal particles by a film of titanium oxide.[12-15] This, in turn, has been shown to be because of the inherent reducibility of titania, especially in the ultra-high vacuum (UHV) treatment environment.[1,16-18]

Recently, O'Shea *et al.*[19] obtained transmission electron microscopy (TEM) images of Co nanoparticles covered by a few atomic layers of TiO_x ($x < 2$) after a reduction treatment (TPR). X-ray photoelectron spectroscopy (XPS) showed that this might be Ti^{3+}. Majzik *et al.*[20] used Auger electron spectroscopy (AES) and scanning tunneling microscopy (STM) to show SMSI on Rh nanoparticles on TiO_2(110). Scanning tunneling microscopy showed ordered decoration of TiO_x on Rh, exhibiting a `wheel structure', which is very similar to that reported for other supported metal systems, such as Pt[14] and Pd islands,[21] and for thin films of oxidized titanium deposited on metal single crystals.[22] This decoration could be removed with a short sputtering procedure[20] (100 s, 0.5 keV). These pinwheel structures have also been observed by Castell on Pd clusters supported on reduced $SrTiO_3$[23] and in TiO_x on Au(111)[24] using STM and Auger. Linsmeier[25] used ISS, XPS and thermal desorption experiments to investigate SMSI after high-temperature reduction

Maney Publishing

treatment. Thermal desorption spectra showed significant CO adsorption on a clean TiO$_2$ sample with Rh nanoparticles (~1 mL), and very little adsorption after SMSI had been induced. X-ray photoelectron spectroscopy showed Ti^{3+} present in the SMSI state. This is in contrast to Bennett *et al.*[21,26] who showed the layer on Pd to be Ti^{2+}-like by using take-off angle variations in XPS, though the effect on CO adsorption[27] was similar to that observed by Linsmeier and Taglauer.[25] Reactivity measurements by Bonanni[28] suggest that high-temperature annealing of Pt on reduced TiO$_2$ results in the encapsulation of Pt by a reduced titania layer, agreeing with a mechanism proposed by Fu *et al.*[29,30]

Materials and methods

All experiments were performed in a UHV system built by Omicron Vacuum Physik capable of performing STM, XPS, low energy ion scattering/ISS and low energy electron diffraction (LEED). The system comprises three separate chambers pumped by a combination of four turbomolecular pumps, three titanium sublimation pumps and two ion pumps, resulting in a base pressure of $<1 \times 10^{-9}$ mbar.

The TiO$_2$ sample was cleaned by Ar$^+$ bombardment at 1 keV, followed by annealing in UHV or oxygen, typically at 773 K, although temperatures in the range 673–873K were used for certain experiments. Surface cleanliness was monitored by XPS and ISS, and gas purity was analyzed using a quadrupole mass spectrometer. X-ray photoelectron spectra were recorded using an Al Kα photon source and an analyzer pass energy of 50 eV unless stated otherwise and were recorded at room temperature. All XPS data were analyzed with CasaXPS[31] and binding energies were calibrated to the O(1 s) peak at 530.4.[32]

The titanium dioxide sample used was a TiO$_2$(110) single crystal (Pi-Kem Ltd. (Salisbury, UK)). The sample was mounted on a standard Omicron molybdenum plate via spot-welded Ta strips. A thermocouple was attached to the sample plate holder for temperature measurement.

Palladium films were grown by metal vapor deposition. The source of Pd was a W filament (0.25 mm, Advent, 99.95%) tightly wrapped with Pd wire (0.125 mm, Goodfellow, 99.95%), which was resistively heated by passing a current of 3A through the coil in UHV.

Results

Sputtering and annealing TiO$_2$(110)

The TiO$_2$(110) surface was prepared in several different ways before the deposition of Pd, Fig. 1, as follows

a.   sputtered at ambient temperature

b.   sputtered then annealed to 873 K for 10 min, and

c.   sputtered then annealed to 873 K in the presence of 2×10^{-6} mbar of O$_2$ for 60 min.

Considering Fig 1*c* first, here the surface is highly oxidized with main peaks at 459 eV and 465 eV binding energy (b.e.) for the 2p$_{3/2,1/2}$ states characteristic of the 4 + oxidation state of Ti. After sputtering at ambient temperature (Fig. 1*a*), the peaks are very poorly defined and broadened on the low b.e. side, characteristic of reduction of the Ti states. This is because of the well-known effect of sputtering on titania surfaces, namely that the lighter atom, the oxygen, is

depleted in the surface relative to Ti.[33] This leaves a much reduced surface, which has mainly Ti$^{3+/2+}$ states present.[1,16,34] After annealing such a surface in vacuum (Fig. 1*b*), the peaks have sharpened up, but nevertheless, when compared with Fig. 1*c*, the surface is clearly still in a considerably reduced state. The Ti^{2+} state is significantly lowered in intensity and the reduced states are now dominated by Ti^{3+}, with peaks at 457.5 and ~462.3 eV. Figure 2 shows the difference spectrum obtained by subtracting the spectrum of the sputter-annealed surface, from that obtained by sputtering (that is, between states c and a above), as detailed in the Supplementary Material. There is loss of intensity of the peaks at ~455.1 and 461.0 eV because of the annealing, consistent with a major component of Ti^{2+} after sputtering, but with some Ti^{3+} too. Figure 3 shows the difference between spectra b and c, indicating the dominance of the 3 + state as the reduced species after annealing the sputtered surface.

Figure 4 is a plot of the effect of annealing on the signals for two of these surfaces, indicating the changes in the oxidized and sputtered states with anneal temperature. Clearly, although annealing in UHV has some oxidative effect, annealing in oxygen, even at such low pressures, is much more effective, as also indicated by the data of Table 1 showing the ISS Ti:O ratios for the three surfaces.

Dosing of Pd

Figure 5 shows the evolution of the Pd$_{3d}$:Ti$_{2p}$ signal ratio, for dosing Pd stepwise onto the three titania surfaces at 300 K (the individual spectra are shown in the Supplementary Material Fig. 1*a–f*). As can be seen, the ratio generally increases in a similar fashion as the coverage increases for the three types of surface. It is important to note that we do not have an independent way of measuring the flux of Pd at the surface and, since these experiments were carried out at different times, with different life history of the filament used, we cannot say with confidence that there is a significant change in morphology of the growing film. That is, the higher ratio of Pd:Ti for the sputtered/annealed layer seen in Fig. 5 could simply be because of a higher flux of Pd at the surface, hence the inset shows a version normalized to the dose time for the sputtered surface. It is clear that the shape is identical for all three curves. The curves indicate an initial period of near linearity (up to ~150 s dosing in the inset), followed by an increased slope, which could indicate initial growth of the Pd as a few monolayers, as proposed by Kaden *et al.*,[35] with multilayer island growth following that initial phase.

Thermal evolution of the Pd layer

The authors then annealed these variously prepared Pd–TiO$_2$ surfaces for 10 min at a variety of temperatures to examine the effect on the Pd and Ti XPS signals, and these data are summarized in Figs. 6 and 7. All the curves show a decrease in the Pd/Ti ratio with increasing temperature, beginning at about 523 K, most likely because of some de-wetting/sintering in the deposited film,[36] followed by a bigger decrease in ratio at higher temperatures. There is little apparent change in the shape or position of the Pd 3d XPS peaks (Fig. 7*b*), but there is a considerable change in the Ti line shape (Fig. 7*a*) with an
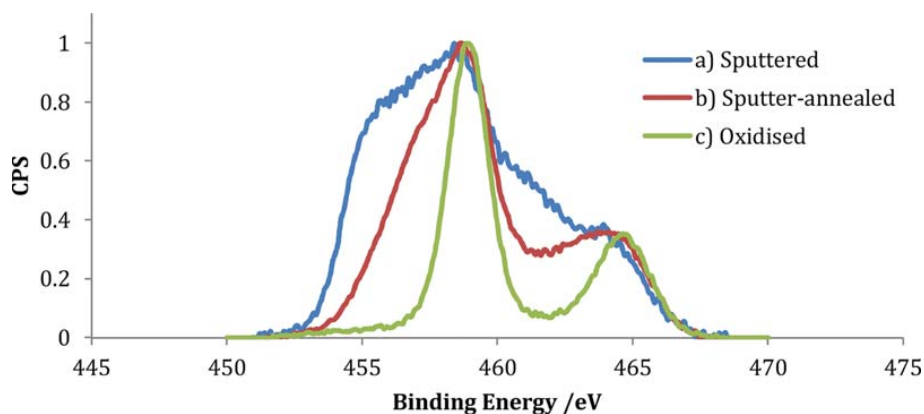
Figure 1 **Normalised Ti 2p spectra from the TiO₂(110) surface after *a* sputtering, *b* sputtering and annealing to 873 K for 10 min and *c* sputtering and then annealing at 873 K in oxygen (2 × 10⁻⁶ mbar) for 60 min**
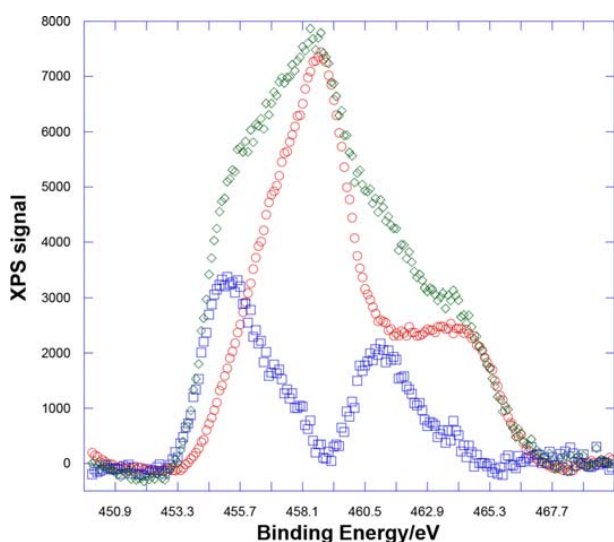

Figure 2 **Showing the difference spectrum (blue curve) between spectrum c (green curve, sputtered surface) and spectrum b (red curve, sputtered surface annealed) in Fig. 1 of the main text. The dominant peaks in the difference spectrum are at 455.3 and 461.0 eV assigned to the Ti²⁺ state**
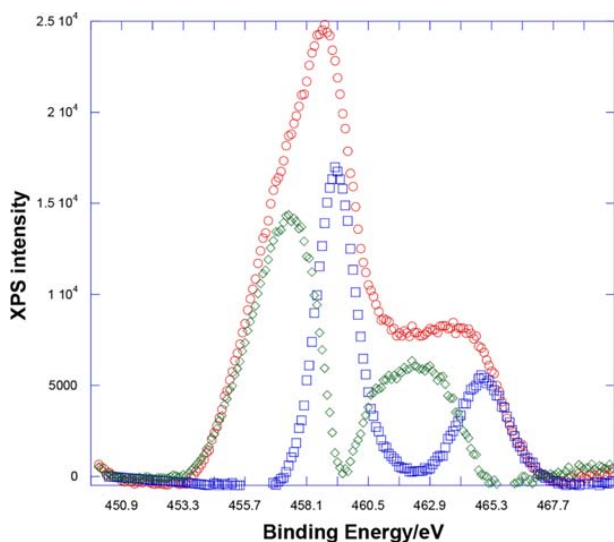

Figure 3 **Showing the difference spectrum (green curve) between spectra b and c in Fig. 1. The dominant peaks are at 457.5 and ~462.5 eV, characteristic of mainly Ti³⁺**
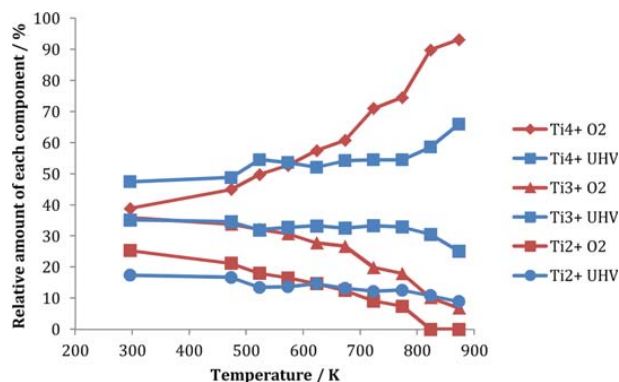

Figure 4 **Variation of the various Ti states as a function of anneal temperature for a sputtered surface being annealed in O₂ and in ultra-high vacuum (UHV), derived from the Ti₂ₚ X-ray photoelectron spectroscopy (XPS)**

Table 1 **Ti/O ion scattering spectroscopy (ISS) integral ratios for the three prepared surfaces**

Surface	Ti/O ISS ratio
Sputtered	2.82
Sputter-annealed	2.72
Oxidized	1.97

increase in the low binding energy, reduced Ti states. However, what we particularly wish to focus on here is the effect seen in Fig. 8, which shows a remarkable decrease in the Pd ISS signal with increasing anneal temperature and an increase in the Ti and O signals. The Pd:Ti ISS ratio decreases by a factor of ∼ 300, largely as a result of the catastrophic loss of Pd signal. Together with this, there is a significant change in the Ti₂ₚ XPS peaks, that is, an increase in intensity at ∼ 456 eV, beginning to occur above 673 K and consistent with the appearance of Ti²⁺ on the surface of the sample. This is the opposite of the behavior observed for the surface without Pd present. The full XPS and ISS data are shown in the Supplementary Material Figs. 2 and 3.

Discussion

TiO₂(110)

It is clear from the above data that the treatment method during surface preparation has a substantial effect on the
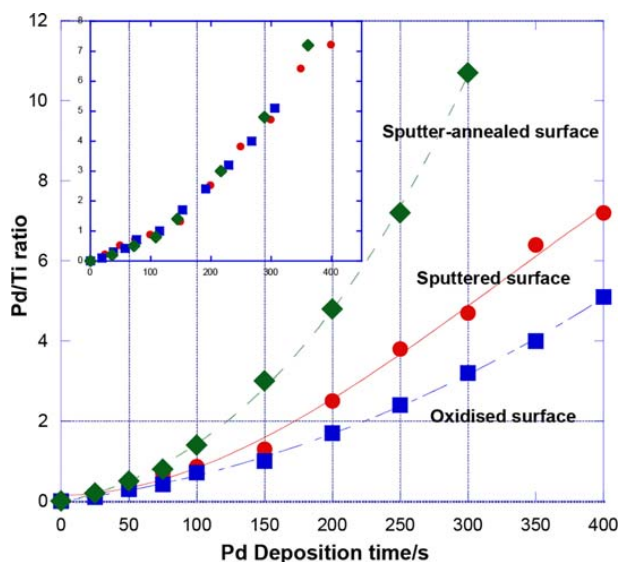
Figure 5 Pd 3d/Ti 2p X-ray photoelectron spectroscopy (XPS) area ratios for each surface during deposition. Red symbols are for deposition onto the sputtered surface, green for the sputter–annealed surface, and blue for the surface sputtered and annealed in oxygen and (inset) normalized to the Pd/Ti ratio for the sputtered surface at 300 s
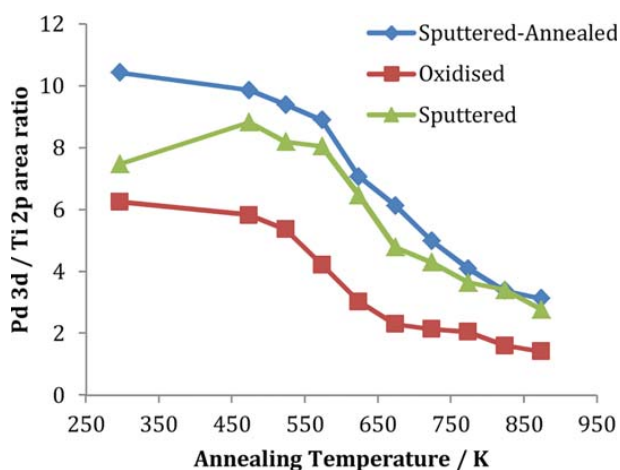

Figure 6   The change in Pd3d/Ti$_{2p}$ area ratio with annealing temperature for the three prepared surfaces

nature of the surface. Sputtering has the effect of removing contaminants from the surface layer, but also removes Ti and O. However, as might be expected, more O is removed during this process and so the Ti:O ratio increases, as seen in Table 1. Concomitant with this, XPS indicates a decrease in the cation charge at the surface, that is, reduction because of the loss of oxygen from the surface. It appears that in the present case these states are mainly Ti^{2+} immediately after sputtering, though after annealing that state diminishes, with an increase in Ti^{3+} and Ti^{4+}. Nolan *et al.*[37] showed that addition of metallic Ti to the TiO$_2$(110) surface results in conversion of that adatom to Ti^{2+} with distribution of the additional electrons around adjacent sites in the adlayer, rather than the formation of only reduced cations immediately beside the anion vacancy, or of polarons. The electrons do not remain located in the anion vacancy for titania, but neither are they itinerant, as might be inferred from the fact
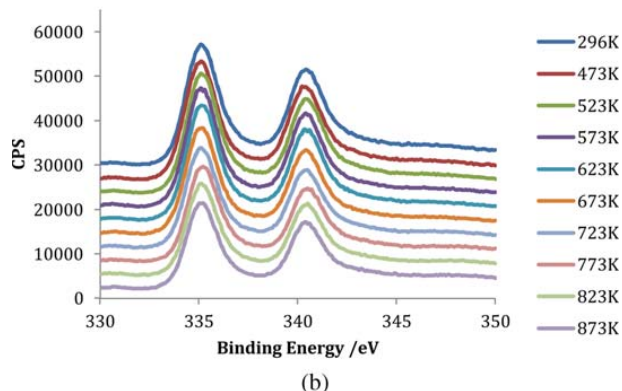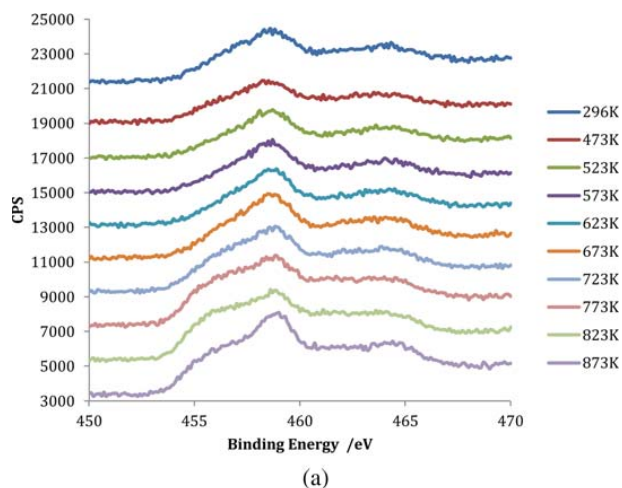

(a)

(b)

Figure 7   *a* The variation in the Ti$_{2p}$ X-ray photoelectron spectroscopy (XPS) signal with increasing temperature for the sputtered surface with Pd post-dosed. *b* The variation in the Pd 3d XPS with increasing anneal temperature for the sputtered surface post-dosed with Pd

that they are d-band (conduction band) electrons. Rather they are located in defect states within the band gap, as shown by Nolan *et al.*[37] However, here we have clearly shown that for a heavily reduced surface low oxidation states are formed, though here the dominant species appears to be Ti^{2+}. Annealing that layer in vacuum results in partial reoxidation of the surface, mainly because of loss of the 2 + state and diffusion of Ti^{3+} into subsurface interstitial sites.[16,21,34]

Table 1 indicates that annealing the sputtered surface has relatively little effect on the Ti:O ratio under these circumstances, but oxidation has a much larger effect. This is owing to the fact that new, stoichiometric titania layers grow over the surface during oxidation, as we showed previously by STM imaging,[16,21,34] occurring by migration of Ti^{3+} from subsurface sites back to the surface.

Pd/TiO$_2$(110)

The authors have previously described the evolution of the structure of Pd films on annealed single crystal TiO$_2$(110) with metal dosing and have shown that the film grows in a Volmer–Weber fashion at ambient temperature,[12,13] that is by nucleation of small nanoparticles, which eventually grow and merge into a holey film.[21,26] After annealing to high temperature such films can be flat[26] and show reasonably good LEED patterns.[21,26] However, annealing to very high-temperature results
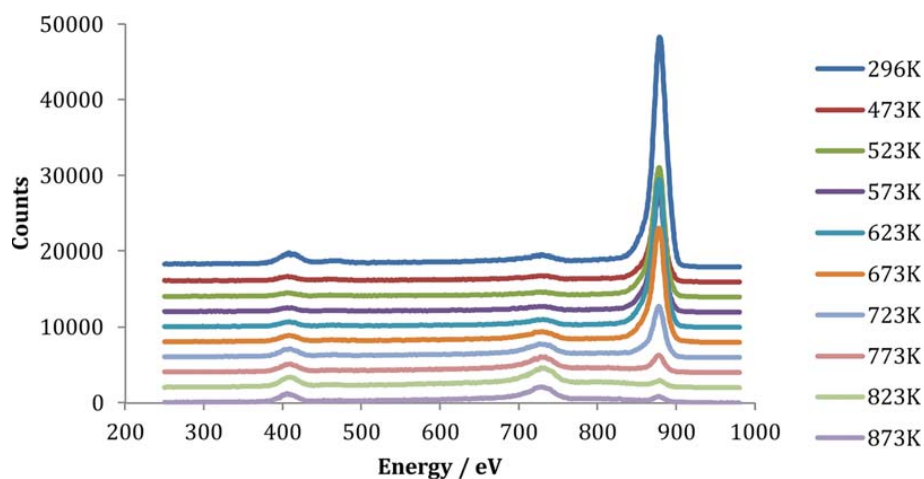
Figure 8 **The effect of heating on the ion scattering spectroscopy (ISS) for the sputtered surface post-dosed with Pd**

in the encapsulation of the metal with a TiO$_x$ film.[21,26] The authors previously proposed that this film on the Pd was TiO-like, since varying the photoelectron take-off angle in XPS indicated that the Ti^{2+} state was dominant at the surface.[21,26,38]

In the present case, we have looked at the effect of pretreating the surface on the growth of the Pd layer and have shown, surprisingly, that the evolution of signal increases in a similar form for the three different surfaces, indicating relatively little change in the growth mode with changes in TiO₂ surface composition.

However, of more interest is the effect of annealing on such samples. What is clearly shown is that an encapsulation layer forms over the Pd particles, beginning at ∼700 K (see Figs. 8 and 9, and Figs. 2 and 3 of Supplementary Material). Here the Pd signal in ISS declines to near zero by ∼800 K, and the Pd:Ti ratio decreases by a factor of ∼300, while in the XPS, the Pd:Ti signal ratio has only declined by ∼60%. Thus, the Pd is still present at the surface of the titania crystal, but has been covered by a layer of TiO$_x$. The XPS confirms an increase in the state at ∼455 eV b.e., associated with Ti^{2+}, and so the encapsulating layer on the Pd appears to be TiO-like, as suggested by the take-off angle results reported previously,[21,26,38] though obviously this layer is also bonded to Pd, and so is unlike bulk TiO.

The effect of encapsulation is seen for all three forms of treatment of the titania surface, Fig. 9. However, what is clear is that it occurs at lower temperature (by ∼80 K) for the sputtered and the sputter–annealed surface than for the oxidized surface. This implies that there are still reduced states in the material even for the oxidized surface, but they reach the surface, and so to the Pd nanoparticles, with more difficulty than for the reduced crystal, which has reduced forms of Ti already at the surface.

Dulub *et al.*[14] carried out similar experiments with Pt on TiO₂ using ISS and STM and also observed SMSI. They dosed ∼25 monolayers of Pd, completely eliminating the Ti signal in ISS and then annealed to >773 K. This caused the Pt signal to disappear from the ISS and the Ti signal to re-appear. Fu *et al.*[30] found a strong dependence of the encapsulation process on the electron density in the conduction band of TiO₂. Encapsulation of Pd clusters was observed on TiO₂ crystals, which were heavily sputtered or reduced, but not on unreduced or slightly sputtered crystals.
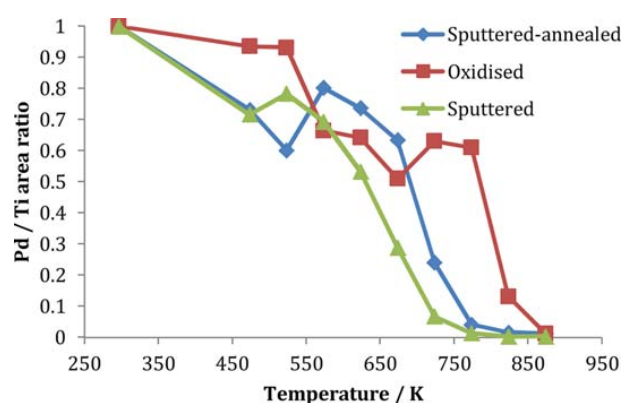

Figure 9 **The change in Pd/Ti ISS ratio against annealing temperature of the three prepared surfaces. Note that in the case of the sputtered surface much more Pd was dosed onto the surface (450 s of dose), compared with 300 s for the annealed and 400 s for the oxidized surface**

In some cases, they found a mix of Ti^{2+} and Ti^{3+} in the XPS after annealing Pd/TiO₂ to 823 K.

It is likely that the encapsulation is strongly related to the state of the reduction of the crystal used in all these cases. Usually, the way the crystal is treated in UHV changes its colour to (at least) pale, transparent blue,[1,34] reflecting the presence of Ti^{3+} in the bulk. In turn this can be useful since the conductivity of the sample increases enormously in such cases,[34] enabling good STM images to be obtained for titania samples. Presumably, there are enough such reduced states in the bulk for our apparently oxidized samples (which are likely to be oxidized in the near-surface region only) to still enable the SMSI effect to occur, even if at higher temperatures, while perhaps in the case of Fu *et al.*[30] this was not the case. Indeed, the authors showed earlier a fourth-order dependence of the oxidation of reduced titania crystals upon the amount of Ti^{3+} in the bulk,[21] which would lead to a dramatic dependence of these effects on the average crystal stoichiometry.

Conclusions

In conclusion, the authors have shown that sputtering of clean TiO₂(110) can result in reduction of the surface such

that Ti^{2+} can dominate the cation states. Thermal annealing results in some reoxidation of the surface layers, especially Ti$^{2+} \rightarrow$ Ti^{3+}, but oxidative treatment is more effective. Surprisingly, the growth mode of Pd on the surface appears to be little affected by the reduction state of the oxide. However, upon annealing of such surfaces, encapsulation of the Pd occurs (the so-called SMSI state), and this is strongly affected by the nature of the oxidation state of the underlying titania surface. This layer is TiO-like.

Conflicts of interest

The authors declare that there are no conflicts of interest.

Acknowledgments

References

1. U. Diebold: *Surf. Sci. Rep.*, 2003, **48**, 53–229.
2. M. Bowker: *Green Chem.*, 2011, **13**, 2235–2246.
3. M. Bowker: *Catal. Lett.*, 2012, **142**, 923–929.
4. A. Kudo and Y. Miseki: *Chem. Soc. Rev.*, 2009, **38**, 253–278.
5. V. Jovic, P. H. Hsieh, W. T. Chen, D. X. Sun-Waterhouse, T. Soehnel and G. I. N. Waterhouse: *Int. J. Nanotechnol.*, 2014, **11**, 686–694.
6. Z. H. N. Al-Azri, V. Jovic, W. T. Chen, D. X. Sun-Waterhouse, J. B. Metson and G. I. N. Waterhouse: *Int. J. Nanotechnol.*, 2014, **11**, 695–703.
7. M. C. Wu, I. C. Chang, W. K. Huang, Y. C. Tu, C. P. Hsu and W. F. Su: *Thin Solid Films*, 2014, **570**, 371–375.
8. M. V. Dozzi, G. L. Chiarello and E. Selli: *J. Adv. Oxid. Technol.*, 2010, **13**, 305–312.
9. R. Su, R. Tiruvalam, A. J. Logsdail, Q. He, C. A. Downing, M. T. Jensen, N. Dimitratos, L. Kesavan, P. P. Wells, R. Bechstein, H. H. Jensen, S. Wendt, C. R. A. Catlow, C. J. Kiely, G. J. Hutchings and F. Besenbacher: *Acs Nano*, 2014, **8**, 3490–3497.
10. M. A. Henderson: *Surf. Sci. Rep.*, 2011, **66**, 185–297.
11. A. A. Ismail and D. W. Bahnemann: *Sol. Energ. Mat. Sol. Cells*, 2014, **128**, 85–101.
12. R. A. Bennett, P. Stone and M. Bowker: *Catal. Lett.*, 1999, **59**, 99–105.
13. R. A. Bennett, P. Stone and M. Bowker: *Faraday Discuss.*, 1999, **114**, 267–277.
14. O. Dulub, W. Hebenstreit and U. Diebold: *Phys. Rev. Lett.*, 2000, **84**, 3646–3649.
15. F. Netzer and S. Surnev: 'Scanning tunneling microscopy in surface science'; 2010, Weinheim, Wiley-VCH.
16. P. Stone, R. Bennett and M. Bowker: *New J. Phys.*, 1999, **1**, 1.1–1.12.
17. M. A. Henderson: *Surf. Sci.*, 1995, **343**, L1156–L1160.
18. M. A. Henderson: *Surf. Sci.*, 1999, **419**, 174–187.
19. V. A. D. O'Shea, M. C. A. Galvan, A. E. P. Prats, J. M. Campos-Martin and J. L. G. Fierro: *Chem. Commun.*, 2011, **47**, 7131–7133.
20. Z. Majzik, N. Balazs and A. Berko: *J. Phys. Chem. C*, 2011, **115**, 9535–9544.
21. R. A. Bennett, C. L. Pang, N. Perkins, R. D. Smith, P. Morrall, R. I. Kvon and M. Bowker: *J. Phys. Chem. B*, 2002, **106**, 4688–4696.
22. G. Barcaro, E. Cavaliere, L. Artiglia, L. Sementa, L. Gavioli, G. Granozzi and A. Fortunelli: *J. Phys. Chem. C*, 2012, **116**, 13302–13306.
23. F. Silly and M. R. Castell: *J. Phys. Chem. B*, 2005, **109**, 12316–12319.
24. C. Wu, M. S. J. Marshall and M. R. Castell: *J. Phys. Chem. C.*, 2011, **115**, 8643–8652.
25. C. Linsmeier and E. Taglauer: *Appl. Catal.*, 2011, **391**, 175–186.
26. M. Bowker, P. Stone, P. Morrall, R. Smith, R. Bennett, N. Perkins, R. Kvon, C. Pang, E. Fourre and M. Hall: *J. Catal.*, 2005, **234**, 172–181.
27. M. Bowker, P. Stone, R. Bennett and N. Perkins: *Surf. Sci.*, 2002, **497**, 155–165.
28. S. Bonanni, K. Ait-Mansour, H. Brune and W. Harbich: *ACS Catal.*, 2011, **1**, 385–389.
29. Q. Fu and T. Wagner: *Surf Sci Rep.*, 2007, **62**, 431–498.
30. Q. Fu, T. Wagner, S. Olliges and H. D. Carstanjen: *J. Phys. Chem. B*, 2005, **109**, 944–951.
31. N. Fairley: 'CasaXPS, Version 2.3.15, Casa Software Ltd, 1999-2011, CasaXPS, Version 2.3.15'; 1999–2011, Casa Software Ltd.
32. U. Diebold and T. Madey: *Surf. Sci. Spectra.*, 1997, **4**, 227–231.
33. R. Kelly and N. Lam: *Radiat. Eff.*, 1973, **19**, 39–48.
34. M. Bowker and R. A. Bennett: *J. Phys. Condens. Matter*, 2009, **21**, 9.
35. W. E. Kaden, T. P. Wu, W. A. Kunkel and S. L. Anderson: *Science*, 2009, **326**, 826–829.
36. R. A. Bennett, D. M. Tarr and P. A. Mulheran: *J. Phys. Condens. Matter*, 2003, **15**, S3139–S3152.
37. M. Nolan, S. D. Elliott, J. S. Mulley, R. A. Bennett, M. Basham and P. Mulheran: *Phys. Rev. B*, 2008, **77**, 235424.
38. M. Bowker and E. Fourre: *Appl. Surf. Sci.*, 2008, **254**, 4225–4229.